



Essential oils from fennel plants as valuable chemical products: gas chromatography–mass spectrometry, FTIR, quantum mechanical investigation, and antifungal activity

Mamoun S. M. Abd El-Kareem¹ · Mohamed A. Rabbih¹ · A. M. Rashad² · Mervat EL-Hefny³

Received: 22 February 2024 / Revised: 10 April 2024 / Accepted: 23 April 2024
© The Author(s) 2024

Abstract

In the present study, the biomass produced by fennel plants (*Foeniculum vulgare* Mill.) was converted to yield bioactive chemicals, and the hydrodistillation method was used to extract the essential oils (EOs) from both the leaves and the umbels. The antifungal activity of the EOs was tested using bioassay against the development of *Fusarium oxysporum* MW854649 and *Alternaria solani* MT279570. Molecular spectroscopic detection techniques were used to evaluate the EO products using gas chromatography–mass spectrometer (GC–MS) and Fourier transform infrared spectroscopy (FTIR). GC–MS equipped with single quadrupole analyzers have been used to measure the electron ionization (EI) mass spectra of the primary constituents of fennel EOs at 70 eV. The main chemical compounds in the EO from leaves were anethole, estragole, D-limonene, trans- β -ocimene, and fenchone, with percentages of 37.94, 35.56, 17.46, 1.53, and 1.49%, respectively. The abundant compounds in the EO from umbels were estragole, anethole, D-limonene, fenchone, and γ -terpinene, with percentages of 51.18, 25.08, 12.22, 6.57, and 2.86%, respectively. EI mass spectral fragmentation of the major compounds D-limonene, estragole, anethole, and fenchone has been investigated. Umbels and leaf EOs at 5000 mg/L displayed the strongest suppression of fungal growth against *A. solani*, with values of 87.78% and 79.63%, respectively, compared to the positive control (94.44%). The EOs from umbels and leaves at 5000 mg/L showed the highest inhibition of fungal growth against *F. oxysporum* as compared to the positive control (94.44%), with values of 77.77% and 72.96%, respectively. All of the important ions—including a few distinctive fragment ions—have comprehensive fragmentation pathways defined. Based on EI, the main routes of fragmentation for the primary compounds have been identified. The existence of alkenes, aliphatic alcohols, ethers, carboxylic acids, ester compounds, alkanes, hydrogen-bonded alcohols, and phenols was demonstrated by the FTIR analysis of fennel EOs. On the other hand, the reactive behavior of the studied molecules has been investigated using two quantum mechanics method: the modified neglect of diatomic overlap (MNDO), a semi-empirical method, and the density functional theory (DFT)/B3LYP hybrid density functional method with the 6-311G (d, p) basis set in the ground state for gas phase. The optimum geometries have been obtained through the execution of computations and electrostatic potential. The obtained analytical and calculated results were then used to understand the activity of the studied EOs in further medical applications.

Keywords Biomass conversion · GC–MS electron · Mass spectra · FTIR · DFT · Fennel oil · Antifungal activity

1 Introduction

The Apiaceae family includes the ancient spice plant fennel (*Foeniculum vulgare* Mill), which is regarded as one of the most significant medicinal herbs in the world [1]. The well-known perennial plant *F. vulgare* is indigenous to the Mediterranean region [2, 3]. It is utilized to prepare herbal drugs [4, 5] and is being utilized for a range of respiratory,

gastrointestinal, and hepatoprotective conditions [6–9]. Research has demonstrated the diuretic, anti-inflammatory, analgesic, and antioxidant properties of herbal medicine preparations [10, 11], ACE inhibition [12], anticancer activities [13–16], and antimicrobial activities [6, 17, 18].

Essential oils (EOs) are the main constituents of fennel seeds and are being used as flavoring agents in various foods, cosmetic, and pharmaceutical products [6, 19, 20]. Estragole (methyl chavicol) was the primary chemical component of fennel seed EOs [21]. It has been observed that *trans*-anethole, fenchone, estragol, and α -phellandrene

Extended author information available on the last page of the article

are the main constituents of *F. vulgare* seed EOs [6]. The content of *trans*-anethole, the main component of the EO, varied between 81.63 and 87.85% according to the maturity stage of fruits [22]. *Trans*-anethole, estragole, fenchone, and D-limonene were highly abundant in the EOs from fennel, with highly antimicrobial against *Aspergillus flavus*, *Candida albicans*, *Bacillus cereus*, and *Staphylococcus aureus* and antioxidant activities [23].

Mass spectrometry (MS) techniques have played a major role in the development of the natural goods industry over the last 5 years. It provided the basis for calculating out the molecular weight and recognizing the identities or structures of most natural compounds [24, 25]. Based on the electron ionization mass spectra of the molecules, the MS methods can yield a great deal of structural information with minimal investment in the molecules under study [26].

The kinetic energy of an ionized molecule is the main factor affecting its capacity to fragment [27]. Moreover, semi-empirical modified neglect of diatomic overlap (MNDO) and density functional theory (DFT) computations are the most efficient means of computing the structure of the substance and supporting the experimental study [28, 29]. These are quantum mechanical techniques that are widely used in chemistry and physics to determine the electronic structure of molecules and their thermochemical properties [30–37]. In this study, the primary constituents of fennel EOs were investigated using the DFT approach. The molecular characteristics, charge distribution, chemical activity, and other significant features of the monomeric components in an EO, i.e., from *Aethionema sancakense* and *Phlomis bruguieri*, can be inferred through DFT calculations [38–43].

Fourier-transform infrared (FTIR) spectroscopy has been used in conjunction with the GC–MS approach because of its capacity to test the quality of EOs in a timely, cost-effective, non-destructive manner [44]. The main advantage of IR is that it requires little to no-sample preparation and may be performed quickly and easily [45, 46]. Previously, mid-infrared spectroscopy was mainly used as a qualitative technique for the verification of quality indicators in distillates or extracts from plants, or for the identification of unknown pure substances by providing structural characterization based on a fingerprint spectrum and functional group vibration [47]. Due to the fact that plant extracts are multicomponent mixtures, IR spectra obtained from them are typically quite complicated [48, 49]. Band assignments may be challenging due to peak overlapping and vibrational mixing; every functional group within a single molecule adds to the overall complexity of the spectrum [50, 51].

Therefore, the main objectives of this study are to use GC–MS to determine the chemical composition of fennel essential oils and to use their electron ionization mass spectra to elucidate the molecular structure of these constituents. Furthermore, DFT and MNDO calculations were

carried out, which included calculating thermodynamic parameters and optimizing geometrical forms. With the aid of the collected data and the experimental data that has been provided, it would be easier to comprehend the bioactivity of the essential oils, which would advance their usage for medicinal and bioactive purposes.

2 Materials and methods

2.1 Plant materials

Two botanical parts (leaves and umbels) from the biomass of fennel plants (*Foeniculum vulgare* Mill) were gathered and identified from plants growing in the nursery of the Department of Floriculture, Ornamental Horticulture, and Garden Design, Faculty of Agriculture (El-Shatby), Alexandria University, Alexandria, Egypt, in May, 2023 (Fig. 1). The plant was identified and vouchered with the number MERV. 0023.

2.2 Extraction of essential oils

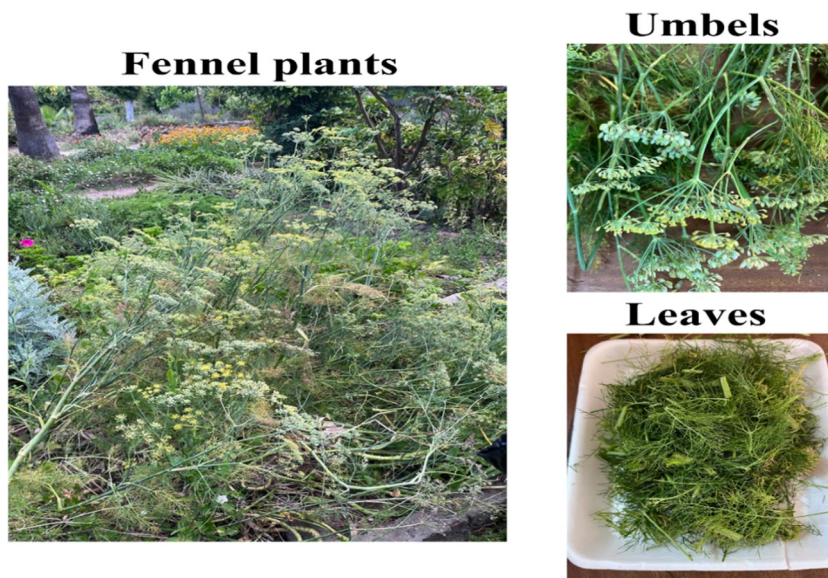
Fresh leaves and umbels of fennel plants each of 250 g were hydro-distilled for 3 h in a Clevenger-style apparatus [38, 52]. Following its separation, anhydrous sodium sulfate (Na_2SO_4) was used to dry the essential oil (EO). EOs were stored at 4 °C in a refrigerator in a sealed Eppendorf tube until further analysis.

2.3 Gas chromatography–mass spectrometry analysis, computational details and FTIR spectral analysis

The EOs from fresh leaves and umbels of fennel plants were analyzed for their chemical compounds using a Facous GC-DSQ mass spectrometer (Thermo Scientific, Waltham, MA, USA) [53]. The geometry of the investigated compounds was optimized based on semi-empirical calculations using the MNDO and Polak–Ribiere conjugated gradient algorithms using the molecular modeling software Hyperchem7.5 (W.Thiel 2003, HyperChemTM, Release 7.5 Pro 200) [54].

Density functional theory (DFT/B3LYP) with 6-311G (d, p) basis set in the ground state for gas phase was used to compute the ground state electrostatic potential (ESP) of the molecule under study [55–57]. Gauss View 05, a molecular visualization application, and the Gaussian 09 program package were used for all of the computations [58]. The spectra investigation of the fennel EOs was recorded using attenuated-total-reflection Fourier transform infrared spectroscopy (ATR-FTIR, Shimadzu IRTracer-100 spectrometer). The IR beam enrolls in the 4000–400 cm^{-1} band and has an incidence angle of 30° [59].

Fig. 1 Biomass of fennel plants and their parts used for the extraction of essential oils



2.4 Antifungal activity of the essential oils

Pure cultures of *Alternaria solani* MT279570 [60] and *Fusarium oxysporum* MW854649 [61] were obtained from a culture that was grown on potato dextrose agar (PDA) for 1 week. A few drops of Tween-80 (0.01%) were added to 0.01% dimethyl sulfoxide (DMSO) to dilute the EOs. To perform the agar dilution procedure, the EOs were added to the agar medium in the various amounts required. From the cultures that were still actively growing, one 5-mm culture disk of each *A. solani* and *F. oxysporum* was taken and put in the center of the Petri dishes. Next, applying the method of poisoned food technique [62], a series of two-fold dilutions of the EOs ranging from 7.5 to 5000 mg/L were made and compared with the reference fungicide, chlorothalonil (0.2 mg/L). The minimum inhibitory concentrations (MICs) of the fungal growth were determined after incubating the Petri dishes at 30 °C for 7 days [63]. Only PDA medium and fungus discs were present in the controls. The growth reduction (%) of the tested two fungi was determined using the following formula: The growth reduction (%) = [(Growth in control – Growth in treatment)/Growth in control] × 100.

2.5 Statistical analysis

A two-way ANOVA analysis of variance (ANOVA) was employed to investigate the effects of the two EOs and their concentrations on the fungal inhibition growth percentages using the STATISTICA program version 8. The data were presented graphically as mean ± SD values and were considered statistically significant when $p < 0.05$.

3 Results and discussion

3.1 The chemical constituents of the essential oils by GC–MS analysis

The chemical components presented in the EO from the leaves of fennel plants are listed in Table 1. The abundant constituents were anethole (37.94%), estragole (35.56%), D-limonene (17.46%), *trans*- β -ocimene (1.53%), and fenchone (1.49%). Table 2 displays the chemical components identified in the EO from the umbels of fennel plants. Estragole (51.18%), anethole (25.08%), D-limonene (12.22%), fenchone (6.57%), and γ -terpinene (2.86%) were the primary components reported for the EO extracted from the umbels of fennel plants. Figure 2 shows the total ion chromatogram recorded by GC–MS of the EO composition of leaves (Fig. 2a) and umbels (Fig. 2b) from fennel plants. Figure 3 displays the chemical structures of the major EO components found in the leaves and umbels of the fennel plants.

3.2 Mass fragmentations of the main compounds

As seen in Fig. 4, the 70-eV mass spectra of the main constituents of the EOs from the leaves and umbels of fennel plants are recorded and analyzed. The peak of the mass spectrum (MS) in the EOs (Fig. 4a) at retention times (RTs) of 10.95 and 10.94 min indicates the anethole component, which is explained by its molecular formula of $C_{10}H_{12}O$. The peak of the molecular ions was noted at m/z 148, with relative intensity (RI) = 100% representing the base peak, and the peak at 147 (RI = 70%). Other

Table 1 The chemical composition of fennel leaf essential oil by GC–MS analysis

Peak	R.T.*	Compound name	Area %	Molecular weight	Molecular formula	R.I.**
1	4.54	β -Pinene	0.24	136	C ₁₀ H ₁₆	979
2	5.29	D-Limonene	17.46	136	C ₁₀ H ₁₆	1030
3	5.41	<i>trans</i> - β -Ocimene	1.53	136	C ₁₀ H ₁₆	1049
4	5.84	γ -Terpinene	0.88	136	C ₁₀ H ₁₆	1060
5	6.21	Fenchone	1.49	152	C ₁₀ H ₁₆ O	1096
6	8.83	Estragole	35.56	148	C ₁₀ H ₁₂ O	1196
7	9.82	Fenchyl acetate	0.62	196	C ₁₂ H ₂₀ O ₂	1223
8	10.96	Anethole	37.94	148	C ₁₀ H ₁₂ O	1286
9	14.59	β -Caryophyllene	0.24	204	C ₁₅ H ₂₄	1419
10	16.01	α -Copaene	0.84	204	C ₁₅ H ₂₄	1432
11	26.44	Estra-1,3,5(10)-trien-17 β -ol	0.57	256	C ₁₈ H ₂₄ O	2259
12	29.16	Phytol	0.59	296	C ₂₀ H ₄₀ O	2114
13	31.53	2,6-Dimethyl-4-[(2,4,6-trimethylphenoxy)methyl]-phenol	0.80	270	C ₁₈ H ₂₂ O ₂	2329
14	33.68	5-[5'-Ethoxy-bicyclo[4.4.1]undeca-1',3',5',7',9'-pentaenylazo)-1h-imidazole-4-carbonitrile	0.90	305	C ₁₇ H ₁₅ N ₅ O	3609

*R.T., retention time (min); **R.I., retention index

Table 2 The chemical composition of fennel umbels essential oil by GC–MS analysis

Peak	R.T.*	Compound name	Area %	Molecular weight	Molecular formula	R.I.**
1	4.54	β -Pinene	0.51	136	C ₁₀ H ₁₆	979
2	5.28	D-Limonene	12.22	136	C ₁₀ H ₁₆	1030
3	5.40	<i>trans</i> - β -Ocimene	0.70	136	C ₁₀ H ₁₆	1049
4	5.84	γ -Terpinene	2.86	136	C ₁₀ H ₁₆	1060
5	6.22	Fenchone	6.57	152	C ₁₀ H ₁₆ O	1096
6	8.88	Estragole	51.18	148	C ₁₀ H ₁₂ O	1196
7	10.94	Anethole	25.08	148	C ₁₀ H ₁₂ O	1286
8	13.62	β -Caryophyllene	0.24	204	C ₁₅ H ₂₄	1419
9	16.01	α -Copaene	0.84	204	C ₁₅ H ₂₄	1432
10	28.83	Phytol	0.32	296	C ₂₀ H ₄₀ O	2114
11	31.53	2,4,6-Tris(dimethylaminomethyl)phenol	0.55	270	C ₁₈ H ₂₂ O ₂	2329
12	33.68	5-[5'-Ethoxy-bicyclo[4.4.1]undeca-1',3',5',7',9'-pentaenylazo)-1h-imidazole-4-carbonitrile	0.90	305	C ₁₇ H ₁₅ N ₅ O	3609

*R.T., retention time (min); **R.I., retention index

significant fragment ions observed were 133 (25%), 121 (42%), 117 (30%), 105 (25%), 91 (21%), and 77 (19%).

The MS of the peak at RTs of 8.88 and 8.83 min (Fig. 4b) represent the estragol component bringing out its chemical formula C₁₀H₁₂O. There was a peak for the molecular ions at m/z 148, with RI = 100% showing the base peak and a peak at 147 (RI = 68%). Other noteworthy fragment ions observed were 133 (20%), 121 (35%), 117 (38%), 105 (22%), 91 (26%), and 77 (25%).

The MS of the peak at RTs of 5.28 and 5.29 min (Fig. 4c) represents the D-limonene component (C₁₀H₁₆). At m/z 136, the molecular ion signal was detected with RI = 21%. The base peak was represented by further notable fragment ions, which were 121 (32%), 107 (30%), 93 (92%), 79 (48%), and 67 (100%).

The chemical formula C₁₀H₁₆O is suggested by the MS of the peak at RTs of 6.22 and 6.21 min (Fig. 4d), which represents the fenchone component. The molecular ion peak

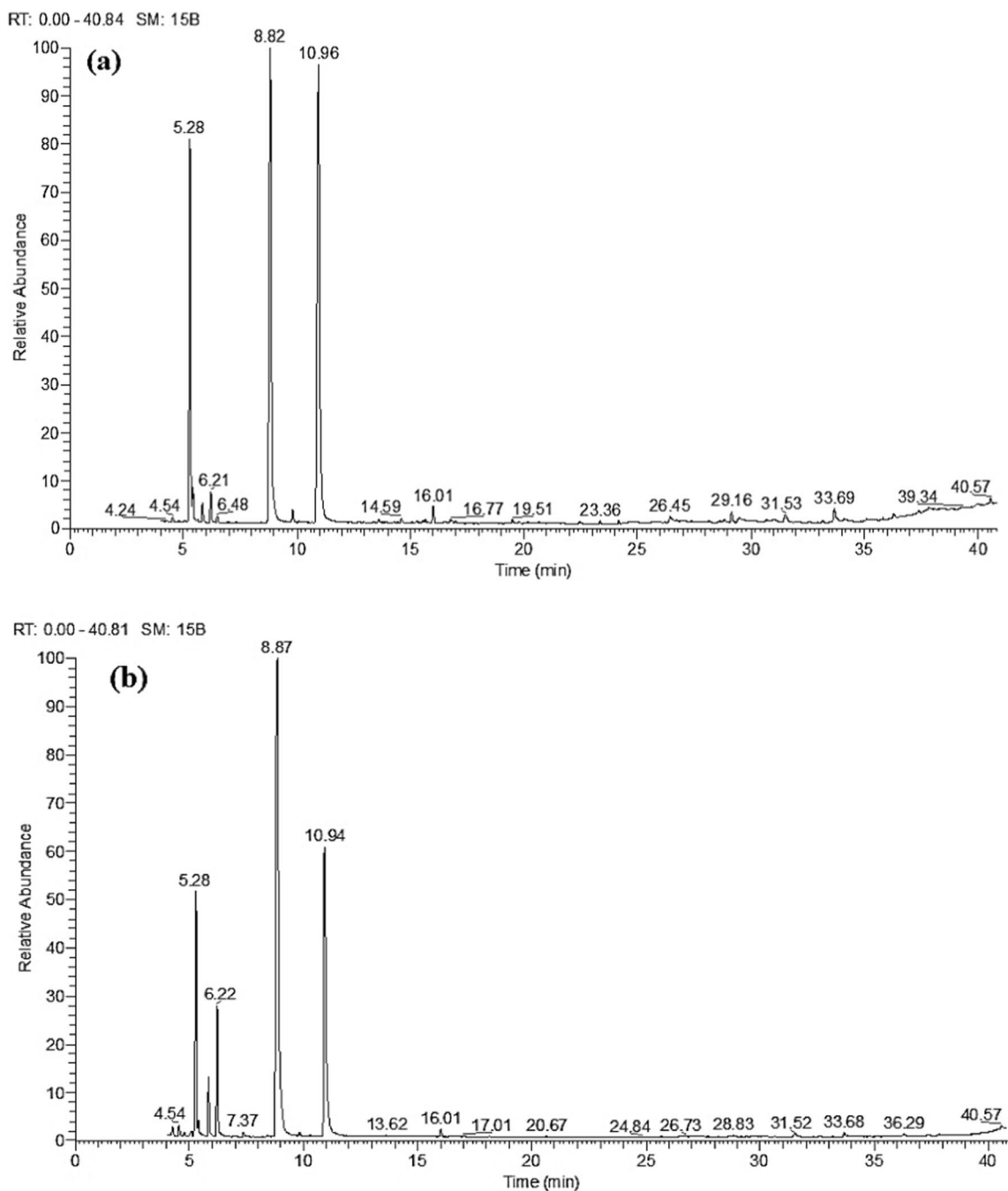


Fig. 2 Total ion chromatogram of the fennel essential oils from leaves (a) and umbels (b) using GC–MS analysis

was observed at m/z 152 with RI=15%. Other notable fragment ions found were 69 with RI (42%), and 81 (100%) represented the base peak.

3.3 Fragmentation pattern of anethole compound

The molecular ion $C_{10}H_{12}O^{+\bullet}$ is obtained from the EI-MS of the anethole compound. This ion exhibited a base peak, and a molecular ion peak at m/z 148 with a high RI (100%)

represents the base peak in the MS. This suggests that this particular molecule is the most stable. The first stage in the fragmentation process of the molecular ion of anethole is the production of the fragment ion at m/z 147 (Fig. 5). The loss of H^\bullet from the molecular ion during the formation of the $[M-H]^{+\bullet}$ ion could be the cause of this occurrence. The molecular ion fragments via three different pathways, each involving the loss of CH_3 to form a different fragment ion: $[M-CH_3]^+$ at m/z 133, $[M-C_2H_3]^+$ at m/z 121 due to the

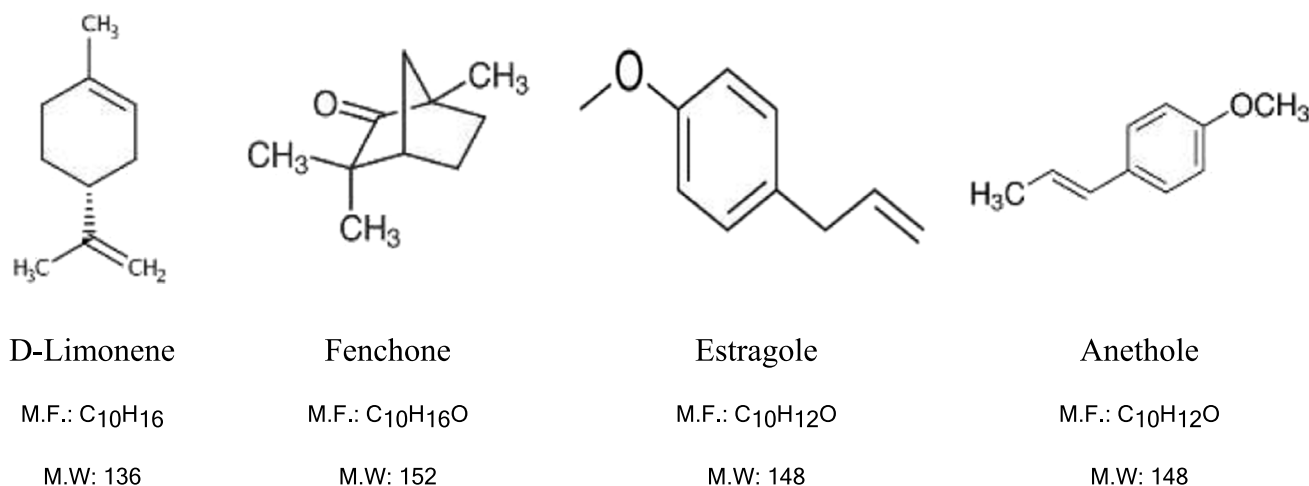


Fig. 3 The chemical structures of the main components with their molecular formula (M.F.) and molecular weight (M.W.) of leaves and umbels fennel essential oils

loss of C₂H₃[•], and [M-CH₃O]⁺ at m/z 117 due to the loss of CH₃O[•], are illustrated in Fig. 5. It is important to note that the estragole compound is an isomer of the molecule anethole and that the MS and primary fragmentation mechanisms of the two compounds are almost the same.

3.4 Fragmentation pattern of D-limonene compound

The molecular ion of C₁₀H₁₆^{+•} is obtained from the EI-MS of D-limonene. The molecular stability of this compound is demonstrated by the MS, which showed a base peak and a molecular ion peak at m/z 136 with RI (31%). The fragmentation process of the D-limonene compound was investigated previously in basil EO with another fragmentation shape [64], as shown in Fig. 6.

3.5 Fragmentation pattern of fenchone compound

The EI-MS of the fenchone gives the molecular ion C₁₀H₁₆O^{+•}, which exhibits a base peak and a molecular ion peak at m/z 152 with RI (22%). This indicates that the molecule has normal stability. The formation of the fragment ion at m/z 81 is the initial step in the fragmentation route of the fenchone molecular ion (Fig. 7), where the production of the [C₆H₉]⁺ ion could account for this. Furthermore, it was observed that the molecular ion fragments at m/z 69 formed the fragment ion [C₄H₅O]⁺.

3.6 Computational details

The optimized molecular geometry of the main components of the EOs is shown in Fig. 8.

Most of the formatted heats are negative, which reflects the strong covalent bonds and lower enthalpy that characterize stable compounds relative to their elements. However, some stable compounds are found to have positive heats of formation, e.g., benzene and the condensed ring of aromatic compounds, making it unwise to generalize from this data alone. The heats of formation therefore permit a precise comparison of the stability of the compounds. The more negative the heat of formation, the greater the stability. Therefore, in the present study, fenchone and anethole compounds have the most negative heat of formation (−39 and −15 kcal/mol) and so they have the highest stability in comparison with the other studied molecules [65].

The thermodynamic data calculated by the MNDO semi-empirical method show that the major components have low heat of formation ($\Delta F(M) = -39$ and -15 kcal/mol for the fenchone and anethole compounds, respectively), and 9.6 and 1.1 kcal/mol for estragole and limonene, respectively. This indicates that fenchone and anethole have higher stability than the other two major components reported in the fennel EOs (Table 3).

3.7 Molecular electrostatic potential (MEP)

Figure 9 displays the molecular electrostatic potential (MEP) plots of the four compounds studied. Because of the high electron density, the areas of this molecule closest to the two oxygen atoms that are linked to the phenolic ring are the most electrophilic sites (red regions). The nucleophilic site of the molecule is shown by the blue patches that are close to the carbon atom.

The molecular charge distribution is not affected by the external test charge. Although MEP is an effective technique for locating reactive sites toward positively or negatively charged

Fig. 4 The 70 eV mass spectra of the leaves and umbels fennel essential oil main components **a** anethole, **b** estragole, **c** D-limonene, and **d** fenchone

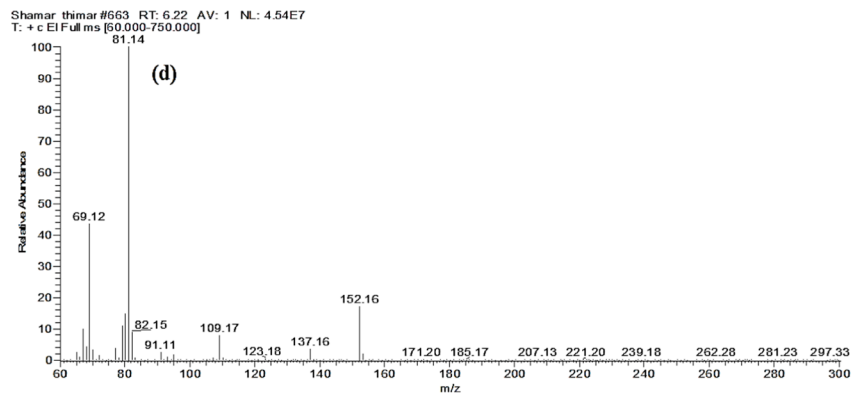
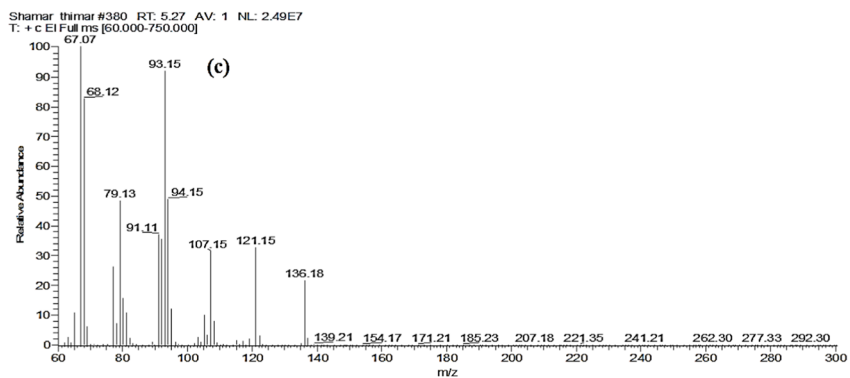
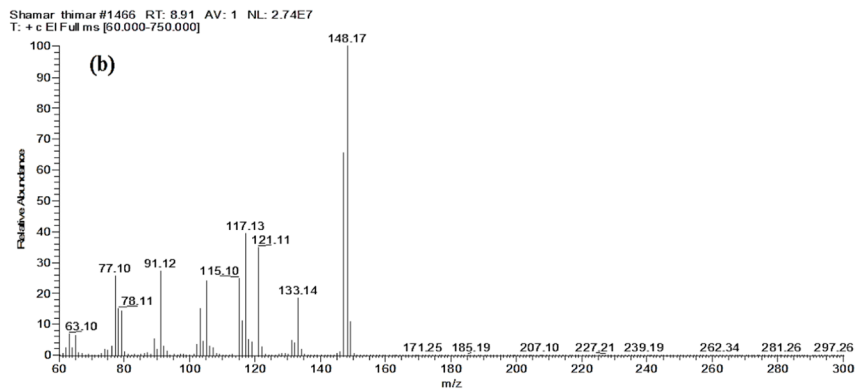
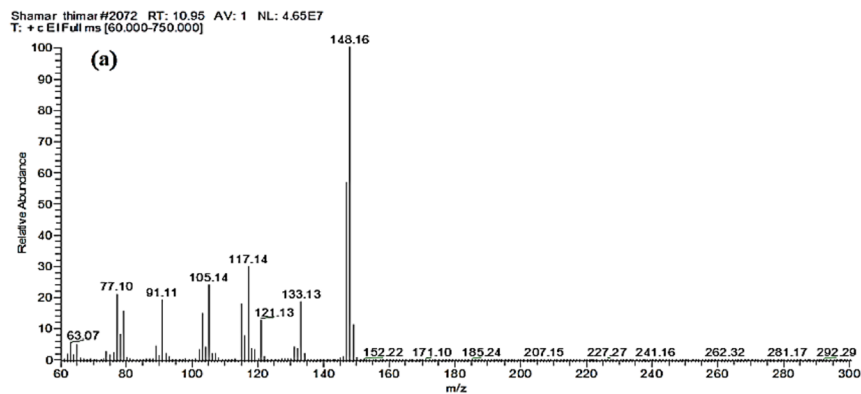


Fig. 5 Electron ionization fragmentation pattern of anethole compound

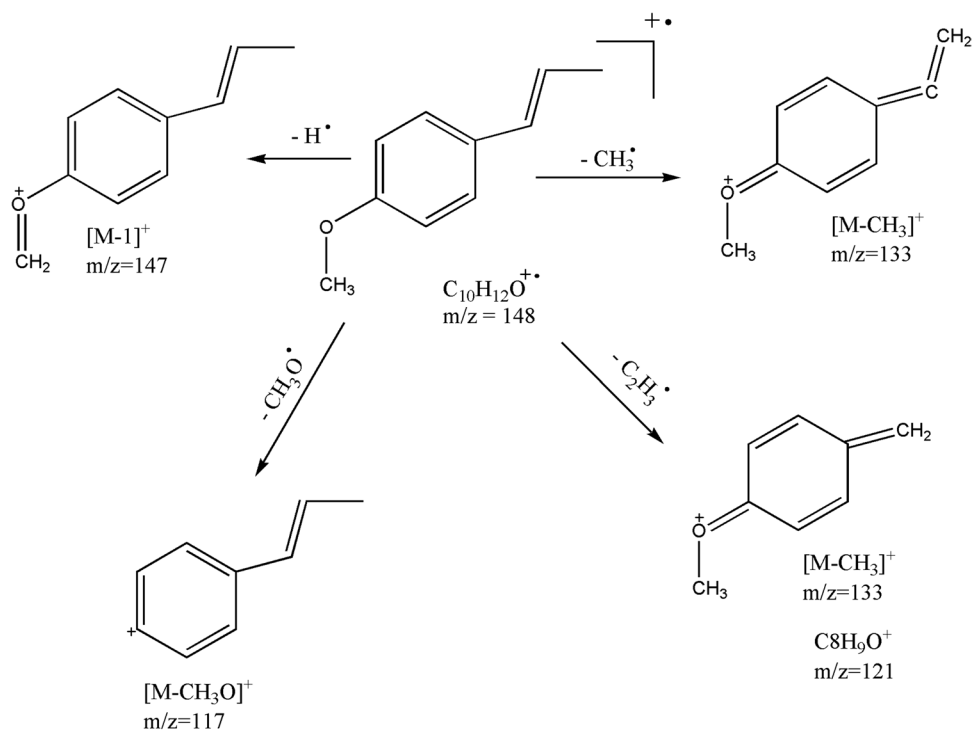


Fig. 6 EI fragmentation pattern of the D-limonene compound

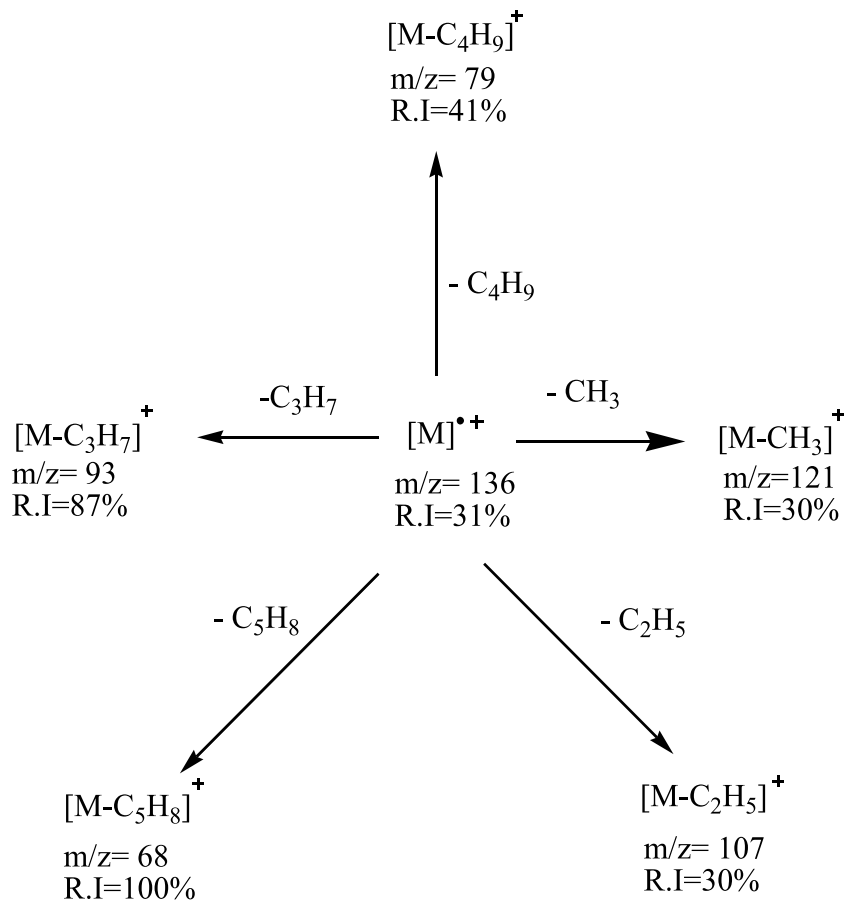
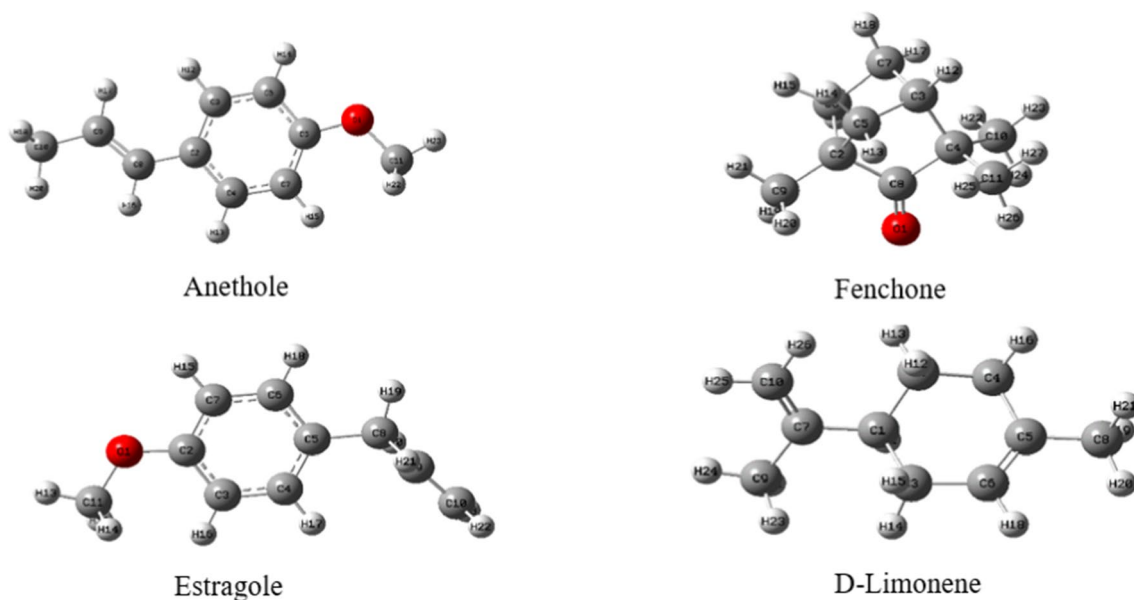
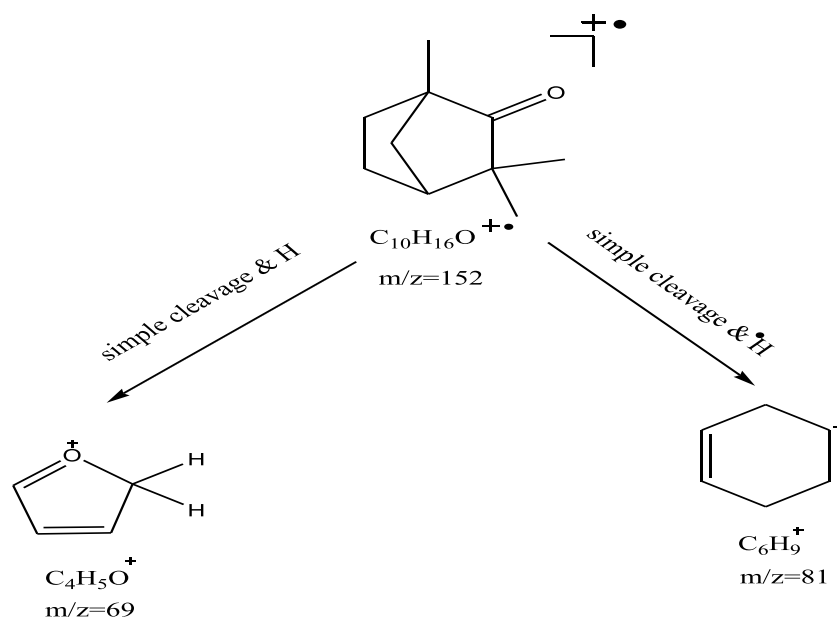


Fig. 7 EI fragmentation pattern of the fenchone compound**Fig. 8** The numbering and optimized geometry structure of the main components of the fennel essential oils**Table 3** Thermochemical data for the studied four major components of the fennel essential oils

Compound	$\Delta_F(M)$ kcal/mol	$\Delta_F(M)^+$ kcal/mol	Dipole. M D
Fenchone	-39	177	2.448
Anethole	-15	164	1.111
Estragole	9.6	179	1.249
D-Limonene	1.1	208	0.132

reactants, it also enables the establishment of hydrogen bonding and structure–activity relationships in the molecule [66]. The dipole moment, electronegativity, and partial charges are strongly correlated with the electrostatic potential, according to quantum chemistry calculations [67]. With the help of a visual representation of the size, shape, charge density, and reactive sites of the molecules on the electrostatic potential energy surface, MEP offers a means of comprehending the relative

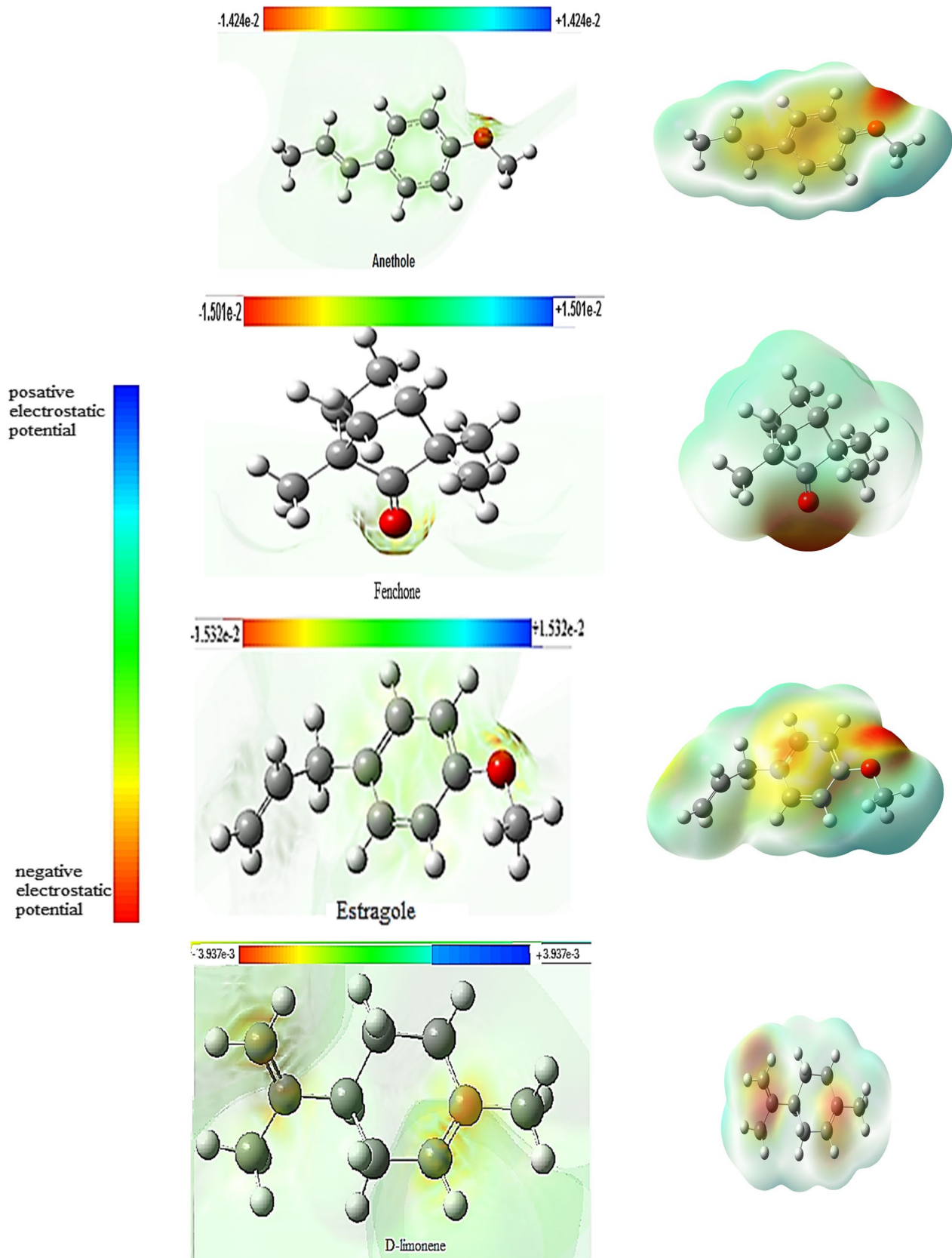


Fig. 9 Electrostatic potential (ESP) and three-dimensional MEP surface maps of the studied molecules

polarity of a molecule [68, 69]. Therefore, it can be proposed a reaction mechanism wherein the oxygen atoms linked to the phenolic ring are targeted intramolecularly by a lone pair of electrons, resulting in a ring closure. The process also involves the transfer of a proton to the negatively charged oxygen atom.

The red- and yellow-colored regions (negative electrostatic potential) on the MEP surface are associated with electrophilic reactivity, while the blue-colored regions (positive electrostatic potential) of MEP are associated with nucleophilic reactivity. Looking at Fig. 9, the oxygen atoms attached to the carboxylic group in anethole, fenchone, and estragole have a negative electron density and are shown in red, while the C5, C6, C7, and C9 in D-limonene have a less negative electron density and are shown in yellow.

Actually, the molecular electrostatic potential (MESP) and the molecular electrostatic potential (MEP) are the same. The charge distributions of molecules are shown in three dimensions by electrostatic potential maps, sometimes referred to as molecular electrical potential surfaces or electrostatic potential energy maps [70, 71]. These maps give us the ability to see a molecule's variable charge areas. Understanding the distribution of charges allows one to determine the interactions between molecules. Three-dimensional diagrams of molecules are highly helpful when it comes to electrostatic potential mapping. They make it possible for us to see the charge distributions and charge-related characteristics of molecules. They also enable us to see the dimensions and forms of molecules. Electrostatic potential maps are very useful in organic chemistry for estimating the behavior of complex compounds [72].

MEP is the net electrostatic effect generated by the total charge distribution (electron + nuclei) of a molecule at a location in space around it. It connects dipole moments, partial charges, electronegativity, and the molecule's site of chemical action to the overall charge distribution. The colors red, blue, and green indicate the varied electrostatic potential values on the surface: red denotes the highest negative electrostatic potential, blue is the highest positive electrostatic potential, and green is the lowest potential [39].

3.8 FTIR measurement

FTIR analysis of the prepared fennel EOs helps to ascertain the possible chemical structure and identify the functional groups of the presented bioactive components [66]. The FTIR spectrum between 500 and 4000 cm^{-1} of diverse fennel EO was recorded, and definite wavenumbers and intensities were recorded and shown in Fig. 10.

The vibrations of the OH groups, carboxyl/carbonyl C=O, C=C, and C-H bending, respectively, can be attributed to the peaks at 3400, 2905, and 2836 cm^{-1} in the FTIR spectra of the EOs from umbels (Fig. 10a) and leaves (Fig. 10b) of fennel plants. This shows that the phenolic, alcoholic, aromatic, and aliphatic components are present. In the FTIR spectrum of

fennel oil, the peaks at 1734, 1609, 1509, and 1454 cm^{-1} correspond to the C=O (ketone), C=C, and aromatic ring, respectively. The presence of C-O, phenol, alcohol, epoxide, and ester as functional groups is indicated by the peaks at 1295, 1242, 1176, 1111, and 1034 cm^{-1} , respectively. The existence of C-H and aromatic rings is indicated by the peaks at 996, 911, 814, 760, 708, 626, and 520 cm^{-1} [67]. All the wavenumbers and transmittances are shown in Tables S1 and S2.

3.9 Antifungal activity of the essential oils

The antifungal activity of the EOs from the leaves and umbels of fennel plants against the growth of *Alternaria solani* is shown in Figs. 11 and 12. Fungal growth inhibitions increased with increasing EO concentrations, whereas entire growth was detected in the control treatment, and full inhibitions were discovered in the positive control (Fig. 11).

Umbels and leaf EOs at 5000 mg/L showed the highest fungal growth inhibition against *A. solani*, with values of $87.78 \pm 1.92\%$ and $79.63 \pm 0.64\%$, respectively, compared to the positive control (94.44%). Additionally, they showed fungal growth inhibition values of $68.15 \pm 1.69\%$ and $66.67 \pm 0.00\%$ at 2500 mg/L, $57.78 \pm 1.11\%$ and $56.67 \pm 0.00\%$ at 1250 mg/L, $50.74 \pm 1.28\%$ and $45.55 \pm 1.115\%$ at 600 mg/L, and $50.74 \pm 1.28\%$ and $45.55 \pm 1.115\%$ at 300 mg/L, respectively (Fig. 12).

Figures 13 and 14 demonstrate the antifungal activity of the EOs from the leaves and umbels of fennel plants against the growth of *Fusarium oxysporum*. The inhibition of fungal growth increased as the EO concentrations increased, while complete inhibitions were found in the positive control and complete growth was observed in the control treatment (Fig. 13).

Umbels and leaf EOs at 5000 mg/L demonstrated the strongest fungal growth inhibition against *F. oxysporum*, with values of $77.77 \pm 3.33\%$ and $72.96 \pm 1.28\%$, respectively, when compared to the positive control (94.44%). Furthermore, they displayed fungal growth inhibition values of $50.74 \pm 1.28\%$ and $44.81 \pm 1.28\%$ at 2500 mg/L, $46.67 \pm 1.11\%$ and $37.40 \pm 2.56\%$ at 1250 mg/L, and $37.41 \pm 0.64\%$ and $24.44 \pm 2.94\%$ at 600 mg/L, respectively (Fig. 14).

The minimum inhibitory concentrations (MIC) for the leaf EOs against *A. solani* and *F. oxysporum* growth were 15 and 30 mg/L, respectively, and for the umbel EO, they were 7.5 and 7.5 mg/L.

From the above results, fennel EOs showed the presence of some bioactive compounds such as anethole, estragole, D-limonene, and fenchone.

Several scientific and biological investigations have focused on the chemical components of fennel EOs. Accordingly, the major components of fennel EO are *trans*-anethole, estragole, fenchone, and D-limonene depending on the chemotype [73–75]. According to Telci et al. [22], *trans*-anethole, a phenylpropanoid, made up the majority of the EO at rates of 84.12% and 87.85% in

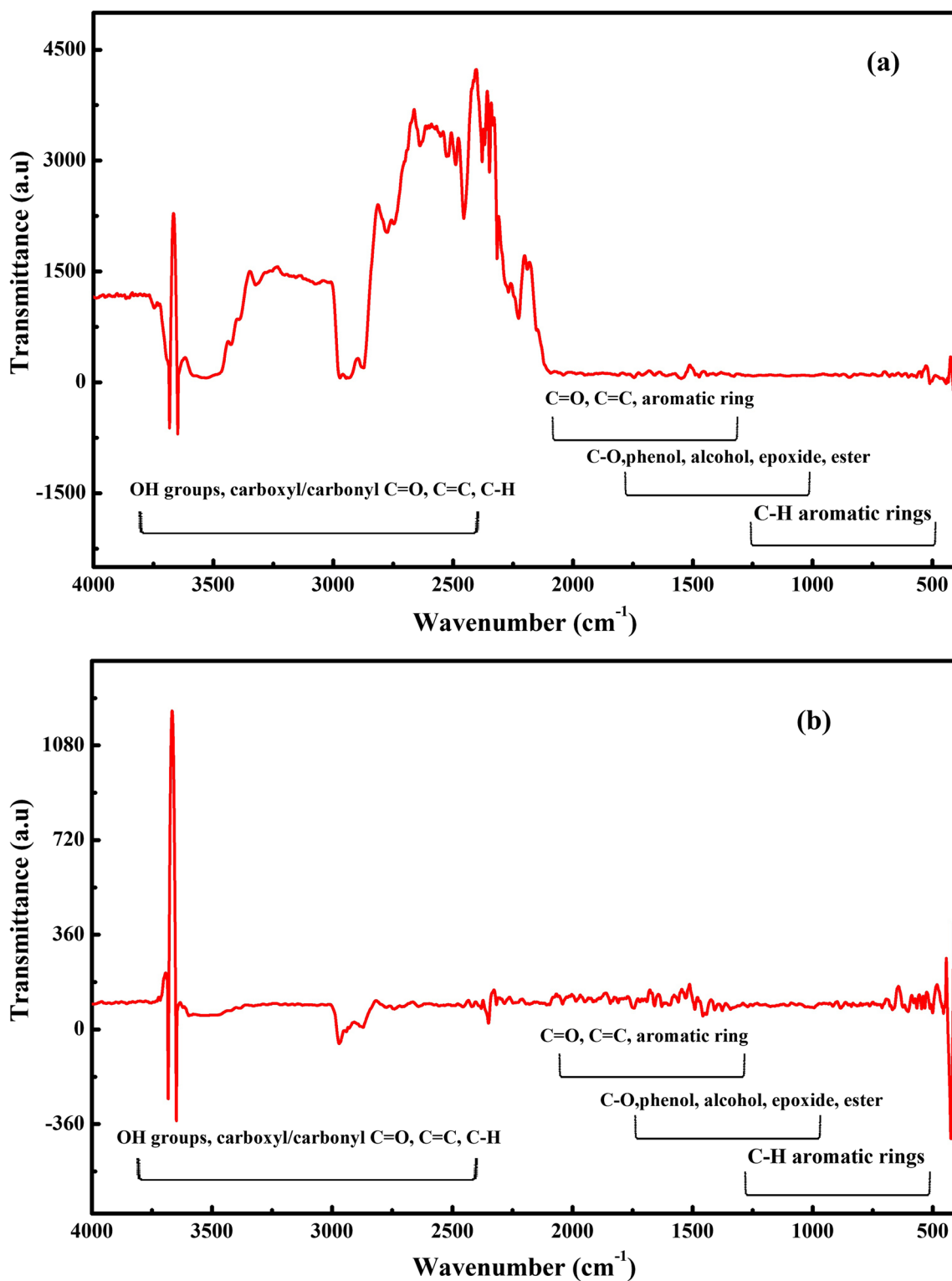


Fig. 10 The experimental FTIR spectra from umbels (a) and leaves (b) of the fennel essential oil

fruits from main umbels and 81.63% and 86.76% in fruits from subsidiary umbels. In another study, *trans*-anethole was shown to be the primary EO component in fennel

[76]. *Trans*-anethole and methyl chavicol are frequently the main ingredients, according to other studies on the EO compositions of various locations [77, 78], though

Fig. 11 The visual observation of the antifungal activity of the essential oils against *Alternaria solani*

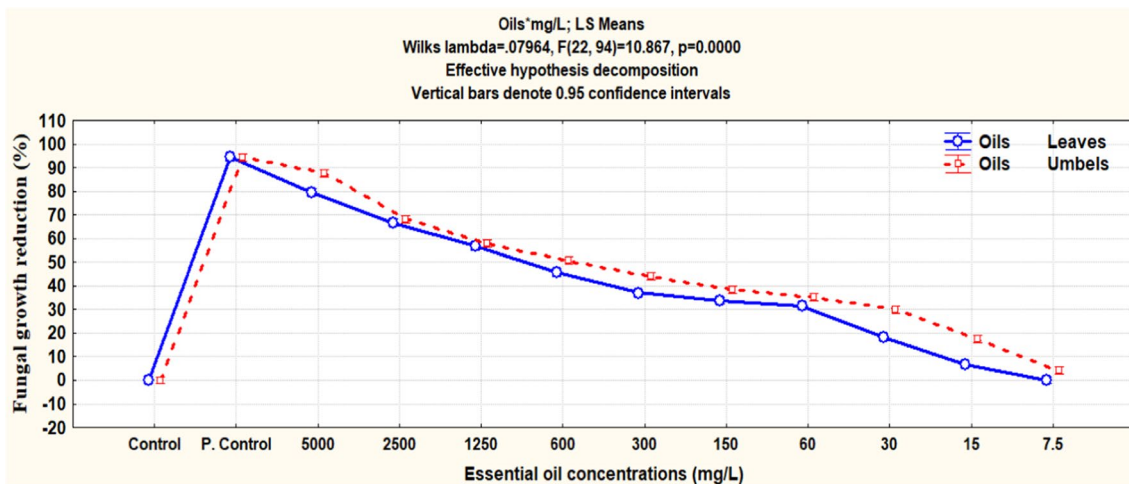
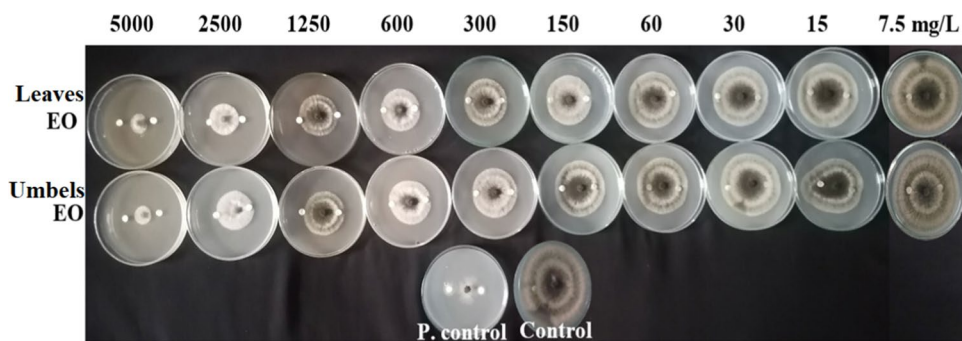
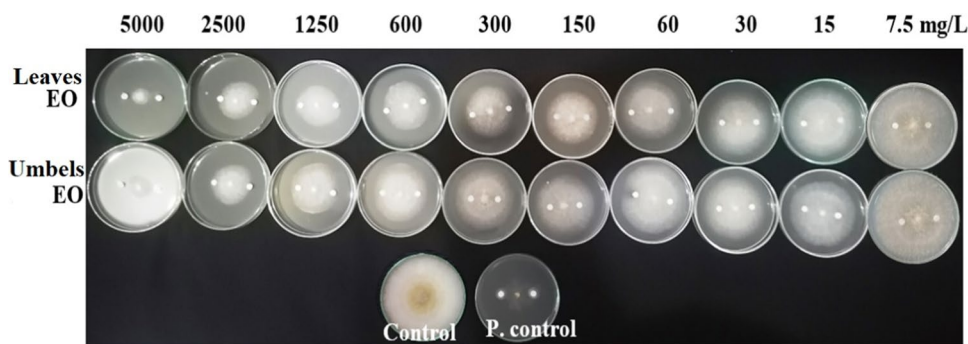


Fig. 12 Antifungal activity of umbels and leaf EOs against *Alternaria solani* at several concentrations compared to positive control (P. control)

Fig. 13 The visual observation of the antifungal activity of the essential oils against *Fusarium oxysporum*



there are different chemotypes of fennel EO that also contain l-fenchone, α -phellandrene, limonene, and α -pinene [76, 79]. Additionally, estragole, fenchone, limonene, and -pinene were present in the EO from the seeds of plants growing in Egypt in percentages of 69.78%, 13.19%, 12.43%, and 2.44%, respectively, as the major components [80].

Significant concentrations of p-cymene (17.5%) and α -pinene (13.4%) were found in the leaf EO, whereas limonene (12.9 and 9.5%) and α -phellandrene (14.6 and

8.7%, respectively) were abundant in the stem and inflorescences. The most common molecule, *trans*-anethole, was present in all samples in trace amounts (traces, 5.3%), whereas fenchone, which occurs often, was only found in modest amounts (3.0%–10.0%) in all samples [3]. The EOs also displayed five chemical groups, including α -phellandrene, methyl chavicol, and *trans*-anethole; α -pinene, limonene, and *trans*-anethole; α -phellandrene; and methyl chavicol and α -pinene [79]. *Trans*-anethole (36.7%), α -ethyl-p-methoxy-benzyl alcohol, *p*-anisaldehyde,

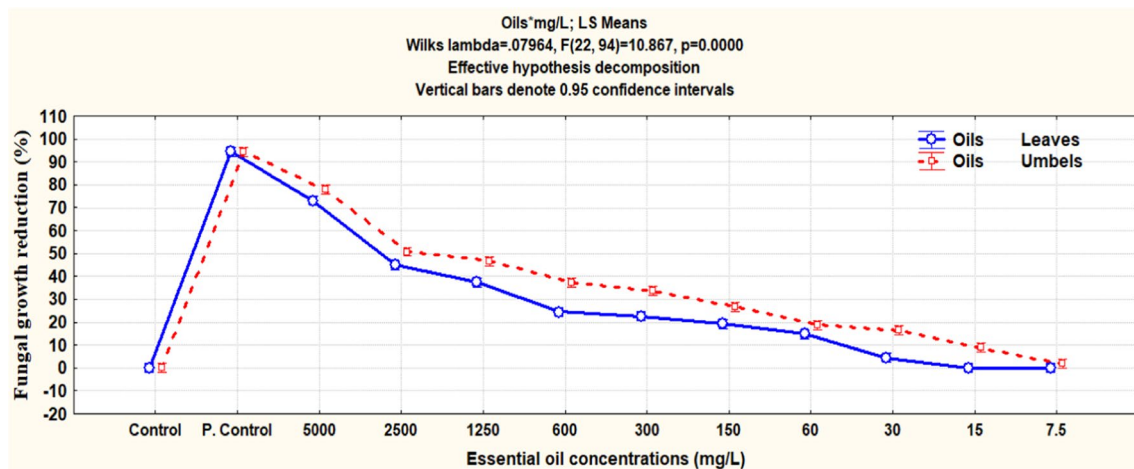


Fig. 14 Antifungal activity of EOs from umbels and leaves of fennels against *Fusarium oxysporum* at several concentrations compared to positive control (P. control)

carvone, 1-phenyl-penta-2,4-diyne, and fenchyl butanoate were the primary constituents of the EO extracted from the aerial parts of fennel in Tajikistan [81]. The main ingredients in the EOs recovered from the dried aerial parts of *F. vulgare* growing in Portugal were trans-anethole (31–36%), α -pinene, and limonene, but estragole (79–88%) dominated in the fruit EO [11]. Estragole (51.04%), limonene, L-fenchone, and trans-anethole were the main ingredients detected in the essential oil of Egyptian fennel seeds; for Chinese fennel seeds, the main components found were trans-anethole (54.26%), limonene, l-fenchone, and estragole [82].

Seed EO revealed the presence of trans-anethole (80.63%), L-fenchone, estragole, and limonene as major compounds and exhibited potential antibacterial activity [13]. Except for *Salmonella* sp., the EOs from dried aerial parts and fruit have shown very little antimicrobial action against *Candida albicans*, *Saccharomyces cerevisiae*, *Staphylococcus aureus*, *Listeria monocytogenes*, and *Bacillus cereus* [11]. Trans-anethole, fenchone, and limonene were identified as the main compounds by the EOs from completely ripened seeds from Iran, which inhibited the growth of *S. epidermidis*, *S. aureus*, *P. aeruginosa*, *E. coli*, and *C. albicans* [17]. Trans-anethol (69.87%), fenchone, estragole, and limonene were found to be the primary chemicals with strong action against *E. coli*, *B. subtilis*, *Aspergillus niger*, *Fusarium solani*, and *Rhizopus solani* in extract extracted from Pakistani fennel seeds [18].

The main compounds found in the EOs extracted from the leaves of 12 populations of *F. vulgare* growing wild in Tunisia were limonene and methyl chavicol, with the Zaghoun population's EOs showing the greatest effectiveness against *Micrococcus luteus* and *S. aureus* [83]. The EOs of three Egyptian fennel cultivars cultivated organically (*Foeniculum vulgare* var. azoricum, *F. vulgare* var. dulce, and *F.*

vulgare var. *vulgare*) showed the presence of trans-anethole, estragole, fenchone, and limonene as abundant compounds in all of the examined EOs. The antimicrobial activity was comparable across all three cultivars [84]. The EOs of seeds exhibited significant concentrations of (E)-anethole, methylchavicol, fenchone, and limonene, which had potent antibacterial effects against *S. aureus*, *Listeria monocytogenes*, *P. aeruginosa*, *Salmonella enteritidis*, and *E. coli* [85]. The main constituents of the EOs extracted from Moroccan wild and cultivated fennel were discovered to be estragole, anethole, and fenchone. The cultivated fennel seeds' EO showed the highest effectiveness against *Salmonella abony*, *P. aeruginosa*, *E. coli*, *B. cereus*, *Staphylococcus aureus*, and *B. subtilis* [86].

Specifically, variations in the chemical makeup of the EOs, particularly the most prevalent components (estragole, limonene, and fenchone), were the cause of the variations in the antifungal activity of *F. vulgare* EO [87, 88]. Among the constituents of this EO, fenchone has shown a moderate level of antifungal activity. *Penicillium funiculosum* and *Trichoderma viride* were more susceptible to the effects of the EO, with a larger percentage of anethol and methyl chavicol (estragole) [87, 89]. The most productive fractions of *F. vulgare* EO were especially high in fenchone, which may have antifungal properties, and estragole [90]. The most efficient EO against gram-positive bacteria was one that was high in estragole [84], and both fenchone and limonene, which are both contained in the EO, have a positive impact on speeding up the healing, anti-inflammatory, and antimicrobial processes [91]. The effectiveness of fennel EO rich in estragole would depend on its combination with other constituents like limonene, fenchone, and trans-anethole [92]. With MIC values of 0.16–0.2–0.25 mg/mL, the EO of *F. vulgare* showed stronger antifungal activity, especially

against *C. albicans*, *Aspergillus niger*, and *A. flavus* [93]. *Ocimum basilicum* EO, with its estragole (65.9%), showed bioactivity as a natural fungicide to manage diseases caused by *F. oxysporum*, *R. solani*, and *A. solani* [94].

Other studies showed that high concentrations of anethole were reported to be poisonous [95]. The secondary metabolites of EOs can freely diffuse through cytoplasmic membranes due to their lipophilic characteristics. Cell death via apoptosis and necrosis can result from this process, which can also impact membrane fluidity and permeability, transport, ion balance, and membrane potential [96, 97].

4 Conclusions

The biomass produced from fennel plants (leaves and umbels) was converted to valuable chemical products of essential oils, which bioassayed against the growth of fungi. This is the first study applying mass spectra, FTIR, and DFT calculations to the Egyptian fennel essential oil. The experimental GC–MS data revealed that the essential oil constituents from the leaves and umbels of fennel plants were anethole, estragol, D-limonene, and fenchone as the major compounds. The obtained mass spectra of these compounds upon electron ionization were verified along with their fragmentation processes. The essential oils from umbel and leaf showed potential antifungal activity against the growth of *A. solani* and *F. oxysporum* according to the reduction of fungal growth and the values of minimum inhibitory concentrations. These experimental data, in conjunction with the FTIR and DFT, provided detailed insights into the chemical behavior of the compounds under study. The theoretical studies, in combination with the experimental data obtained along with the works, may influence the understanding of some interactions and properties of natural compounds in the medical, chemical, and biological applications in the future.

Supplementary Information The online version contains supplementary material available at <https://doi.org/10.1007/s13399-024-05675-2>.

Author contribution M.E.-H. collected the plant sample, essential oils extraction, chemical analysis, and antifungal activity; M.S.M. Abd E.-K., M.A.R., and A.M.R. did the laboratory works about chemical analysis, gas chromatography–mass spectrometry, FTIR, and quantum mechanics investigations. All authors have equal contributions to writing the manuscript. All authors read and approved the final manuscript.

Funding Open access funding provided by The Science, Technology & Innovation Funding Authority (STDF) in cooperation with The Egyptian Knowledge Bank (EKB).

Data availability All data generated or analyzed during this study are included in this published article.

Declarations

Ethics approval and consent to participate Not applicable.

Consent for publication Not applicable.

Competing interests The authors declare no competing interests.

Open Access This article is licensed under a Creative Commons Attribution 4.0 International License, which permits use, sharing, adaptation, distribution and reproduction in any medium or format, as long as you give appropriate credit to the original author(s) and the source, provide a link to the Creative Commons licence, and indicate if changes were made. The images or other third party material in this article are included in the article's Creative Commons licence, unless indicated otherwise in a credit line to the material. If material is not included in the article's Creative Commons licence and your intended use is not permitted by statutory regulation or exceeds the permitted use, you will need to obtain permission directly from the copyright holder. To view a copy of this licence, visit <http://creativecommons.org/licenses/by/4.0/>.

References

1. Abebie B, Engeda D, Wondimagegn M (2017) Phytochemical screening, antioxidant and antimicrobial activities of seeds of *Foeniculum vulgare* (ensilal). World J Pharm Res 5(3):198–208
2. Bahmani K, Darbandi AI, Ramshini HA, Moradi N, Akbari A (2015) Agro-morphological and phytochemical diversity of various Iranian fennel landraces. Ind Crops Prod 77:282–294. <https://doi.org/10.1016/j.indcrop.2015.08.059>
3. Manolakou S, Pitarokili D, Koliopoulos G, Michaelakis A, Tzakou O (2008) Essential oil composition of different parts of Greek *Foeniculum vulgare* and larvicidal activity of the stem oil. Planta Med 74(09):PI15. <https://doi.org/10.1055/s-0028-1084923>
4. Azeez S (2008) Fennel. In: Parthasarathy VA, Chempakam B, Zachariah TJ (eds) Chemistry of spices. CABI, Wallingford, pp 227–241
5. Weiss EA (2002) Umbelliferae. In: Weiss EA (ed) Spice crops. CAB International, Wallingford, UK, pp 284–298
6. Rather MA, Dar BA, Sofi SN, Bhat BA, Qurishi MA (2016) *Foeniculum vulgare*: a comprehensive review of its traditional use, phytochemistry, pharmacology, and safety. Arab J Chem 9:S1574–S1583. <https://doi.org/10.1016/j.arabjc.2012.04.011>
7. Badgujar SB, Patel VV, Bandivdekar AH (2014) *Foeniculum vulgare* mill: a review of its botany, phytochemistry, pharmacology, contemporary application, and toxicology. Biomed Res Int 2014:842674. <https://doi.org/10.1155/2014/842674>
8. Rafeian F, Amani R, Rezaei A, Karaça AC, Jafari SM (2023) Exploring fennel (*Foeniculum vulgare*): composition, functional properties, potential health benefits, and safety. Crit Rev Food Sci Nutr 19:1–18. <https://doi.org/10.1080/10408398.2023.2176817>
9. Jadid N, Widodo AF, Ermavitalini D, Sa'adah NN, Gunawan S, Nisa C, (2023) The medicinal Umbelliferae plant Fennel (*Foeniculum vulgare* Mill): cultivation, traditional uses, phytopharmacological properties, and application in animal husbandry. Arab J Chem 16(3):104541. <https://doi.org/10.1016/j.arabjc.2023.104541>
10. Choi E-M, Hwang J-K (2004) Antiinflammatory, analgesic and antioxidant activities of the fruit of *Foeniculum vulgare*. Fitoterapia 75(6):557–565. <https://doi.org/10.1016/j.fitote.2004.05.005>
11. Miguel MG, Cruz C, Faleiro L, Simões MTF, Figueiredo AC, Barroso JG, Pedro LG (2010) *Foeniculum vulgare* essential oils: chemical composition, antioxidant and antimicrobial activities. Nat Prod Commun 5(2):1934578X1000500231. <https://doi.org/10.1177/1934578X1000500231>
12. Chaudhary SK, Maity N, Nema NK, Bhadra S, Saha BP, Mukherjee PK (2013) Angiotensin converting enzyme inhibition activity of fennel and coriander oils from India. Nat Prod Commun

- 8(5):1934578X1300800531. <https://doi.org/10.1177/1934578X1300800531>
13. Akhbari M, Kord R, Jafari Nodooshan S, Hamed S (2019) Analysis and evaluation of the antimicrobial and anticancer activities of the essential oil isolated from *Foeniculum vulgare* from Hamedan. Iran Nat Prod Res 33(11):1629–1632. <https://doi.org/10.1080/14786419.2017.1423310>
 14. Suleiman WB, Helal EE-H (2022) Chemical constituents and potential pleiotropic activities of *Foeniculum vulgare* (Fennel) ethanolic extract; in vitro approach. Egypt J Chem 65(7):617–626. <https://doi.org/10.21608/ejchem.2021.107991.4938>
 15. Kaveh R, Naghmachi M, Motaghi MM, Amirmahani F, Danaei M (2022) Antibacterial and antioxidant activities and anticancer effects of fennel seeds (*Foeniculum vulgare*) against lung cancer cells. Proc Nat Acad Sci, India Sect B: Biol Sci. <https://doi.org/10.1007/s40011-022-01390-y>
 16. Noreen S, Tufail T, Badar Ul Ain H, Awuchi CG (2023) Pharmacological, nutraceutical, functional and therapeutic properties of fennel (*Foeniculum vulgare*). Int J Food Prop 26(1):915–927. <https://doi.org/10.1080/10942912.2023.2192436>
 17. Ghasemian A, Al-Marzoqi A-H, Mostafavi SKS, Alghanimi YK, Teimouri M (2020) Chemical composition and antimicrobial and cytotoxic activities of *Foeniculum vulgare* mill essential oils. J Gastrointest Cancer 51(1):260–266. <https://doi.org/10.1007/s12029-019-00241-w>
 18. Anwar F, Ali M, Hussain AI, Shahid M (2009) Antioxidant and antimicrobial activities of essential oil and extracts of fennel (*Foeniculum vulgare* Mill) seeds from Pakistan. Flavour Fragr J 24(4):170–176. <https://doi.org/10.1002/ffj.1929>
 19. Gori L, Gallo E, Mascherini V, Mugelli A, Vannacci A, Firenzuoli F (2012) Can estragole in fennel seed decoctions really be considered a danger for human health? A fennel safety update. Evid Based Complement Alternat Med 2012:860542. <https://doi.org/10.1155/2012/860542>
 20. Javed R, Hanif MA, Ayub MA, Rehman R (2020) Chapter 19 - Fennel. In: Hanif MA, Nawaz H, Khan MM, Byrne HJ (eds) Medicinal Plants of South Asia. Elsevier, pp 241–256. <https://doi.org/10.1016/B978-0-08-102659-5.00019-7>
 21. Moustafa MAM, Amer A, Al-Shuraym LA, Ibrahim E-DS, El-Hefny DE, Salem MZM, Sayed S (2022) Efficacy of chemical and bio-pesticides on cowpea aphid, *Aphis craccivora*, and their residues on the productivity of fennel plants (*Foeniculum vulgare*). J King Saud Univ Sci 34(3):101900. <https://doi.org/10.1016/j.jksus.2022.101900>
 22. Telci I, Demirtas I, Sahin A (2009) Variation in plant properties and essential oil composition of sweet fennel (*Foeniculum vulgare* Mill) fruits during stages of maturity. Indu Crops Prod 30(1):126–130. <https://doi.org/10.1016/j.inducrop.2009.02.010>
 23. Roby MHH, Sarhan MA, Selim KA-H, Khalel KI (2013) Antioxidant and antimicrobial activities of essential oil and extracts of fennel (*Foeniculum vulgare* L.) and chamomile (*Matricaria chamomilla* L.). Indu Crops Prod 44:437–445. <https://doi.org/10.1016/j.inducrop.2012.10.012>
 24. Bouslimani A, Sanchez LM, Garg N, Dorrestein PC (2014) Mass spectrometry of natural products: current, emerging and future technologies. Nat Prod Rep 31(6):718–729. <https://doi.org/10.1039/C4NP00044G>
 25. Salem MZM, El-Hefny M, Ali HM, Elansary HO, Nasser RA, El-Settawy AAA, El-Shanhorey N, Ashmawy NA, Salem AZM (2018) Antibacterial activity of extracted bioactive molecules of *Schinus terebinthifolius* ripened fruits against some pathogenic bacteria. Microb Pathogen 120:119–127. <https://doi.org/10.1016/j.micpath.2018.04.040>
 26. Hu X, Zheng Y, Sun J, Shang L, Wang G, Zhang H (2009) Simultaneous quantification of benazepril, gliclazide and valsartan in human plasma by LC–MS–MS and application for rapidly measuring protein binding interaction between rhein and these three drugs. Chromatographia 69(9):843–852. <https://doi.org/10.1365/s10337-009-1017-z>
 27. Bourcier S, Hoppilliard Y (2003) Fragmentation mechanisms of protonated benzylamines. electrospray ionisation-tandem mass spectrometry study and ab initio molecular orbital calculations. Eur J Mass Spectrom (Chichester) 9(4):351–360. <https://doi.org/10.1255/ejms.566>
 28. Bredow T, Jug K (2005) Theory and range of modern semiempirical molecular orbital methods. Theor Chem Acc 113(1):1–14. <https://doi.org/10.1007/s00214-004-0610-3>
 29. Cojocaru C, Rotaru A, Harabagiu V, Sacarescu L (2013) Molecular structure and electronic properties of pyridylindolizine derivative containing phenyl and phenacyl groups: comparison between semi-empirical calculations and experimental studies. J Mol Struct 1034:162–172. <https://doi.org/10.1016/j.molstruc.2012.08.027>
 30. Husch T, Reiher M (2018) Comprehensive analysis of the neglect of diatomic differential overlap approximation. J Chem Theory Comput 14(10):5169–5179. <https://doi.org/10.1021/acs.jctc.8b00601>
 31. Husch T, Vaucher AC, Reiher M (2018) Semiempirical molecular orbital models based on the neglect of diatomic differential overlap approximation. Int J Quantum Chem 118(24):e25799. <https://doi.org/10.1002/qua.25799>
 32. Gieseking RLM, Ratner MA, Schatz GC (2018) Benchmarking semiempirical methods to compute electrochemical formal potentials. J Phys Chem A 122(33):6809–6818. <https://doi.org/10.1021/acs.jpca.8b05143>
 33. Almutairi MS, Soumya S, Al-Wabli RI, Joe IH, Attia MI (2018) Density functional theory calculations, vibration spectral analysis and molecular docking of the antimicrobial agent 6-(1,3-benzodioxol-5-ylmethyl)-5-ethyl-2-[[2-(morpholin-4-yl)ethyl] sulfanyl] pyrimidin-4(3H)-one. Open Chem 16(1):653–666. <https://doi.org/10.1515/chem-2018-0067>
 34. Sundaraganesan N, Dominic Joshua B (2007) Vibrational spectra and fundamental structural assignments from HF and DFT calculations of methyl benzoate. Spectrochim Acta - A: Mol Biomol Spectrosc 68(3):771–777. <https://doi.org/10.1016/j.saa.2006.12.059>
 35. Ong AWW, Cao SY, Kwek LC (2023) An improved parameterization procedure for NDDO-descendant semi-empirical methods. J Mol Model 29(4):118. <https://doi.org/10.1007/s00894-023-05499-3>
 36. Behiry SI, Nasser RA, Abd El-Kareem SM, M, Ali HM, Salem MZM, (2020) Mass spectroscopic analysis, MNDO quantum chemical studies and antifungal activity of essential and recovered oil constituents of lemon-scented gum against three common molds. Processes 8(3):275. <https://doi.org/10.3390/pr8030275>
 37. Ali HM, Elgat WAA, El-Hefny M, Salem MZM, Taha AS, Al Farraj DA, Elshikh MS, Hatamleh AA, Abdel-Salam EM (2021) New approach for using of *Mentha longifolia* L. and *Citrus reticulata* L. essential oils as wood-biofungicides: GC-MS, SEM, and MNDO quantum chemical studies. Materials 14(6):1361. <https://doi.org/10.3390/ma14061361>
 38. Demirpolat A, Akman F, Kazachenko AS (2022) An experimental and theoretical study on essential oil of *Aethionema sancakense*: characterization, molecular properties and RDG analysis. Molecules 27(18):6129. <https://doi.org/10.3390/molecules27186129>
 39. Akman F, Demirpolat A, Kazachenko AS, Kazachenko AS, Issaoui N, Al-Dossary O (2023) Molecular structure, electronic properties, reactivity (ELF, LOL, and Fukui), and NCI-RDG studies of the binary mixture of water and essential oil of *Phlomis bruguieri*. Molecules 28(6):2684. <https://doi.org/10.3390/molecules28062684>

40. Akman F (2023) Effect of solvents on intra- and inter-molecular interactions of oligothiophenes. *J Mol Model* 29(9):276. <https://doi.org/10.1007/s00894-023-05684-4>
41. Akman F (2017) Molecular structure, kinetics and mechanism of thermal decomposition, molecular electrostatic potential, thermodynamic parameters and HOMO–LUMO analysis of coumarin-containing graft copolymer. *Polym Bull* 74(8):2975–2993. <https://doi.org/10.1007/s00289-016-1875-0>
42. Akman F (2016) Experimental and theoretical investigation of molecular structure, vibrational analysis, chemical reactivity, electrostatic potential of benzyl methacrylate monomer and homopolymer. *Can J Phys* 94(9):853–864. <https://doi.org/10.1139/cjp-2016-0252>
43. Akman F (2015) Density functional theory (DFT) and Hartree-Fock (HF) calculations of potential p-vinylbenzyl chloride-based macroinitiator for atom transfer radical polymerization. *Can J Phys* 94(3):290–304. <https://doi.org/10.1139/cjp-2015-0665>
44. Baranska M, Schulz H, Reitzenstein S, Uhlemann U, Strehle MA, Krüger H, Quilitzsch R, Foley W, Popp J (2005) Vibrational spectroscopic studies to acquire a quality control method of *Eucalyptus* essential oils. *Biopolym* 78(5):237–248. <https://doi.org/10.1002/bip.20284>
45. Beć KB, Grabska J, Huck CW (2020) Biomolecular and bioanalytical applications of infrared spectroscopy – a review. *Anal Chim Acta* 1133:150–177. <https://doi.org/10.1016/j.aca.2020.04.015>
46. Baker MJ, Trevisan J, Basso P, Bhargava R, Butler HJ, Dorling KM, Fielden PR, Fogarty SW, Fullwood NJ, Heys KA, Hughes C, Lasch P, Martin-Hirsch PL, Obinaju B, Sockalingum GD, Sulé-Suso J, Strong RJ, Walsh MJ, Wood BR, Gardner P, Martin FL (2014) Using Fourier transform IR spectroscopy to analyze biological materials. *Nat Protoc* 9(8):1771–1791. <https://doi.org/10.1038/nprot.2014.110>
47. Coates J (2000) Interpretation of infrared spectra, a practical approach. In: Meyers RA, McKelvy ML (eds) *Encyclopedia of analytical chemistry: applications, theory and instrumentation*. John Wiley & Sons, Ltd, Chichester. <https://doi.org/10.1002/9780470027318.a5606>
48. Agatonovic-Kustrin S, Ristivojevic P, Gegechkori V, Litvinova TM, Morton WD (2020) Essential oil quality and purity evaluation via ft-ir spectroscopy and pattern recognition techniques. *Appl Sci* 10(20):7294. <https://doi.org/10.3390/app10207294>
49. Sasidharan S, Chen Y, Saravanan D, Sundram K, Latha LY (2011) Extraction, isolation and characterization of bioactive compounds from plants' extracts. *Afr J Tradit Complement Altern Med* 8(1):1–10. <https://doi.org/10.4314/ajtcam.v8i1.60483>
50. Baiz CR, Błasiak B, Bredenbeck J, Cho M, Choi J-H, Corcelli SA, Dijkstra AG, Feng C-J, Garrett-Roe S, Ge N-H, Hanson-Heine MWD, Hirst JD, Jansen TLC, Kwac K, Kubarych KJ, Londergan CH, Maekawa H, Reppert M, Saito S, Roy S, Skinner JL, Stock G, Straub JE, Thielges MC, Tominaga K, Tokmakoff A, Torii H, Wang L, Webb LJ, Zanni MT (2020) Vibrational spectroscopic map, vibrational spectroscopy, and intermolecular interaction. *Chem Rev* 120(15):7152–7218. <https://doi.org/10.1021/acs.chemrev.9b00813>
51. Barone V, Alessandrini S, Biczysko M, Cheeseman JR, Clary DC, McCoy AB, DiRisio RJ, Neese F, Melosso M, Puzzarini C (2021) Computational molecular spectroscopy. *Nat Rev Methods Primers* 1(1):38. <https://doi.org/10.1038/s43586-021-00034-1>
52. Mohareb ASO, Elashmawy MAA, Nawar MEM, Abdelrahman AK, Ahmed FM, Hassona AEA, Salem MZM (2023) Chemical compositions and antifungal activity of *Corymbia citriodora*, *Cupressus macrocarpa*, and *Syzygium cumini* extracts: GC–MS and HPLC analysis of essential oils and phenolic compounds. *Biomass Conver Bioref*. <https://doi.org/10.1007/s13399-023-05106-8>
53. Abd El-Kareem MS, Rabbih MA, Elansary HO, Al-Mana FA (2020) Mass spectral fragmentation of *Pelargonium graveolens* essential oil using GC–MS semi-empirical calculations and biological potential. *Processes* 8(2):128. <https://doi.org/10.3390/pr8020128>
54. Abd El-Kareem MS, El-desawy M, Hawash M, Fahmey M (2018) Structural investigation of sparfloxacin drug using mass spectrometry and MNDO semi-empirical molecular orbital calculations. *Int J Adv Chem* 6(1):74–78. <https://doi.org/10.14419/ijac.v6i1.9177>
55. Ditchfield R, Hehre WJ, Pople JA (1971) Self-consistent molecular-orbital methods. IX. An extended Gaussian-type basis for molecular-orbital studies of organic molecules. *J Chem Phys* 54(2):724–728. <https://doi.org/10.1063/1.1674902>
56. Becke AD (1992) Density-functional thermochemistry. I. The effect of the exchange-only gradient correction. *J Chem Phys* 96(3):2155–2160. <https://doi.org/10.1063/1.462066>
57. Frisch A, Foresman J (1996) *Exploring chemistry with electronic structure methods*. Gaussian, Inc., Pittsburgh, 354 pp. <https://acta-arhiv.chem-soc.si/50/50-1-159.pdf>
58. Frisch A, Nielson A, Holder A (2000) *Gaussview user manual*. Gaussian Inc, Pittsburgh, PA, p 556
59. Pavia DL, Lampman GM, Kriz GS, Vyvyan JA (2014) *Introduction to spectroscopy*, 5th edn. Cengage Learning, 786 pp. https://www.hdki.hr/_download/repository/Pavia-Introduction-to-Spectroscopy%5B1%5D.pdf
60. Mohamed AA, Salah MM, El-Dein MMZ, EL-Hefny M, Ali HM, Farraj DAA, Hatamleh AA, Salem MZM, Ashmawy NA (2021) Ecofriendly bioagents, *Parthenocissus quinquefolia*, and *Plectranthus neochilus* extracts to control the early blight pathogen (*Alternaria solani*) in tomato. *Agronomy* 11(5):911. <https://doi.org/10.3390/agronomy11050911>
61. Shakam HM, Mohamed AA, Salem MZM (2022) Down-regulatory effect of essential oils on fungal growth and Tri4 gene expression for some *Fusarium oxysporum* strains: GC-MS analysis of essential oils. *Arch Phytopathol Plant Prot* 55(8):951–972. <https://doi.org/10.1080/03235408.2022.2064081>
62. Gupta M, Sharma S, Bhadauria R (2015) Fungitoxic activity of fruit extracts of *Syzygium cumini* (L) Skeels against plant pathogenic fungi *Alternaria alternata* and *Fusarium oxysporum*. *Arch Phytopathol Plant Prot* 48(4):354–364. <https://doi.org/10.1080/03235408.2014.888875>
63. Kottearachchi NS, Sammani A, Kelaniyangoda DB, Samarasekara R (2012) Anti-fungal activity of essential oils of Ceylon *Eucalyptus* species for the control of *Fusarium solani* and *Sclerotium rolfsii*. *Arch Phytopathol Plant Prot* 45(17):2026–2035. <https://doi.org/10.1080/03235408.2012.720469>
64. Abd El-Kareem MS, Rabbih MAEF, Selim ETM, Elsherbiny EAE-m, El-Khateeb AY, (2016) Application of GC/EIMS in combination with semi-empirical calculations for identification and investigation of some volatile components in basil essential oil. *Int J Anal Mass Spectrom Cromatogr* 4(1):14–25. <https://doi.org/10.4236/ijamsc.2016.41002>
65. Li B, Li L, Wang Y (2020) Theoretical calculations about the thermal stability and detonation character of nitramino-substituted pyrrole. *Química Nova* 43(3):325–328. <https://doi.org/10.21577/0100-4042.20170496>
66. Dager A, Uchida T, Maekawa T, Tachibana M (2019) Synthesis and characterization of mono-disperse carbon quantum dots from fennel seeds: photoluminescence analysis using machine learning. *Sci Rep* 9(1):14004. <https://doi.org/10.1038/s41598-019-50397-5>
67. Chen G, Wu S, Hui L, Zhao Y, Ye J, Tan Z, Zeng W, Tao Z, Yang L, Zhu Y (2016) Assembling carbon quantum dots to a layered carbon for high-density supercapacitor electrodes. *Sci Rep* 6(1):19028. <https://doi.org/10.1038/srep19028>
68. Ganiev B, Mardonov U, Kholikova G (2023) Molecular structure, HOMO-LUMO, MEP – analysis of triazine compounds using

- DFT (B3LYP) calculations. Mater Today: Proc. <https://doi.org/10.1016/j.matpr.2023.09.191>
69. Abraham CS, Prasana JC, Muthu S (2017) Quantum mechanical, spectroscopic and docking studies of 2-amino-3-bromo-5-nitropyridine by density functional method. Spectrochim Acta - A: Mol Biomol Spectrosc 181:153–163. <https://doi.org/10.1016/j.saa.2017.03.045>
 70. Murray JS, Sen K (1996) Molecular electrostatic potentials: concepts and applications
 71. Scrocco E, Tomasi J (1973) The electrostatic molecular potential as a tool for the interpretation of molecular properties. In: New concepts II. Topics in current chemistry Fortschritte der Chemischen Forschung, vol 42. Springer, Berlin, Heidelberg. https://doi.org/10.1007/3-540-06399-4_6
 72. Mamy L, Patureau D, Barriuso E, Bedos C, Bessac F, Louchart X, Martin-laurent F, Miege C, Benoit P (2015) Prediction of the fate of organic compounds in the environment from their molecular properties: a review. Crit Rev Environ Sci Technol 45(12):1277–1377. <https://doi.org/10.1080/10643389.2014.955627>
 73. Aprotosoae AC, Spac A, Hancianu M, Miron A, Tanasescu VF, Dorneanu V, Stanescu U (2010) The chemical profile of essential oils obtained from fennel fruits (*Foeniculum vulgare* Mill.). Farmacia 58(1):46–53
 74. Radulović NS, Blagojević PD (2010) A note on the volatile secondary metabolites of *Foeniculum vulgare* Mill. (Apiaceae). FU Phys Chem Tech 8(1):25–37. <https://doi.org/10.2298/FUPCT1001025R>
 75. Stefanini M, Ming L, Marques M, Facanali R, Meireles M, Moura L, Marchese J, Sousa L (2006) Essential oil constituents of different organs of fennel (*Foeniculum vulgare* var. *vulgare*). Rev Bras Pl Med, Botucatu 8:193–198
 76. Díaz-Maroto MC, Pérez-Coello MS, Esteban J, Sanz J (2006) Comparison of the volatile composition of wild fennel samples (*Foeniculum vulgare* Mill.) from Central Spain. J Agric Food Chem 54(18):6814–6818. <https://doi.org/10.1021/jf0609532>
 77. Miraldi E (1999) Comparison of the essential oils from ten *Foeniculum vulgare* Miller samples of fruits of different origin. Flavour Fragr J 14(6):379–382. [https://doi.org/10.1002/\(SICI\)1099-1026\(199911/12\)14:6%3c379::AID-FFJ833%3e3.0.CO;2-8](https://doi.org/10.1002/(SICI)1099-1026(199911/12)14:6%3c379::AID-FFJ833%3e3.0.CO;2-8)
 78. Barazani O, Cohen Y, Fait A, Diminshtein S, Dudai N, Ravid U, Putievsky E, Friedman J (2002) Chemotypic differentiation in indigenous populations of *Foeniculum vulgare* var *vulgare* in Israel. Biochem Syst Ecol 30(8):721–731. [https://doi.org/10.1016/S0305-1978\(02\)00019-4](https://doi.org/10.1016/S0305-1978(02)00019-4)
 79. Piccaglia R, Marotti M (2001) Characterization of some Italian types of wild fennel (*Foeniculum vulgare* Mill.). J Agric Food Chem 49(1):239–244. <https://doi.org/10.1021/jf000636+>
 80. Cavaleiro CMF, Roque OL, da Cunha AP (1993) Contribution for the characterization of Portuguese fennel chemotypes. J Essent Oil Res 5(2):223–225. <https://doi.org/10.1080/10412905.1993.9698207>
 81. Sharopov F, Valiev A, Satyal P, Gulmurodov I, Yusufi S, Setzer WN, Wink M (2017) Cytotoxicity of the essential oil of fennel (*Foeniculum vulgare*) from Tajikistan. Foods 6(9). <https://doi.org/10.3390/foods6090073>
 82. Ahmed AF, Shi M, Liu C, Kang W (2019) Comparative analysis of antioxidant activities of essential oils and extracts of fennel (*Foeniculum vulgare* Mill.) seeds from Egypt and China. Food Sci Hum Wellness 8(1):67–72. <https://doi.org/10.1016/j.fshw.2019.03.004>
 83. Khammassi M, Ayed RB, Loupasaki S, Amri I, Hanana M, Hamrouni L, Jamoussi B, Khaldi A (2023) Chemical diversity of wild fennel essential oils (*Foeniculum vulgare* Mill.): a source of antimicrobial and antioxidant activities. S Afr Bot 153:136–146. <https://doi.org/10.1016/j.sajb.2022.12.022>
 84. Shahat AA, Ibrahim AY, Hendawy SF, Omer EA, Hammouda FM, Abdel-Rahman FH, Saleh MA (2011) Chemical composition, antimicrobial and antioxidant activities of essential oils from organically cultivated fennel cultivars. Molecules 16(2):1366–1377. <https://doi.org/10.3390/molecules16021366>
 85. Ben Abdesslem S, Boulares M, Elbaz M, Ben Moussa O, St-Gelais A, Hassouna M, Aider M (2021) Chemical composition and biological activities of fennel (*Foeniculum vulgare* Mill.) essential oils and ethanolic extracts of conventional and organic seeds. J Food Process Preserv 45(1):e15034. <https://doi.org/10.1111/jfpp.15034>
 86. Abdellaoui M, Bouhlali EdT, Derouich M, El-Rhaffari L (2020) Essential oil and chemical composition of wild and cultivated fennel (*Foeniculum vulgare* Mill.): a comparative study. S Afr J Bot 135:93–100. <https://doi.org/10.1016/j.sajb.2020.09.004>
 87. Mimica-Dukić N, Kujundžić S, Soković M, Couladis M (2003) Essential oil composition and antifungal activity of *Foeniculum vulgare* Mill. obtained by different distillation conditions. Phytother Res 17(4):368–371. <https://doi.org/10.1002/ptr.1159>
 88. Aamir F, Bashir H, Mahmood M (2018) Antifungal activity of freshly growing seeds of fennel (*Foeniculum vulgare*). Pak J Med Health Sci 12(4):1487–1489
 89. Mota AS, Martins MR, Arantes S, Lopes VR, Bettencourt E, Pombal S, Gomes AC, Silva LA (2015) Antimicrobial activity and chemical composition of the essential oils of Portuguese *Foeniculum vulgare* fruits. Nat Prod Commun 10(4). <https://doi.org/10.1177/1934578X1501000437>
 90. Garzoli S, Božović M, Baldisserotto A, Sabatino M, Cesa S, Pepi F, Vicentini CB, Manfredini S, Ragno R (2018) Essential oil extraction, chemical analysis and anti-Candida activity of *Foeniculum vulgare* Miller – new approaches. Nat Prod Res 32(11):1254–1259. <https://doi.org/10.1080/14786419.2017.1340291>
 91. Keskin I, Gunal Y, Ayla S, Kolbasi B, Sakul A, Kilic U, Gok O, Koroglu K, Ozbek H (2017) Effects of *Foeniculum vulgare* essential oil compounds, fenchone and limonene, on experimental wound healing. Biotech Histochem 92(4):274–282. <https://doi.org/10.1080/10520295.2017.1306882>
 92. Kazemi M, Mousavi E, Kharestani H (2012) Chemical compositions and antimicrobial activities of essential oils of *Varthemia persica*, *Foeniculum vulgare* and *Ferula lycia*. Curr Res Bacteriol 5(2):42–52
 93. Belabdeli F, Piras A, Bekhti N, Falconieri D, Belmokhtar Z, Merad Y (2020) Chemical composition and antifungal activity of *Foeniculum vulgare* mill. Chem Afr 3(2):323–328. <https://doi.org/10.1007/s42250-020-00130-x>
 94. Hamad YK, Abobakr Y, Salem MZM, Ali HM, Al-Sarar AS, Al-Zabib AA (2019) Activity of plant extracts/essential oils against three plant pathogenic fungi and mosquito larvae: GC/MS analysis of bioactive compounds. BioResour 14(2):4489–4511. <https://doi.org/10.15376/biores.14.2.4489-4511>
 95. Van Wyk B-E, Wink M (2018) Medicinal plants of the world. CABI, London, 520 pp
 96. Wink M (2008) Evolutionary advantage and molecular modes of action of multi-component mixtures used in phytomedicine. Curr Drug Metabol 9(10):996–1009. <https://doi.org/10.2174/138920008786927794>
 97. Bhardwaj P, Alok U, Khanna A (2013) In vitro cytotoxicity of essential oils: a review. Int J Res Pharm Chem 3(3):675–681

Publisher's Note Springer Nature remains neutral with regard to jurisdictional claims in published maps and institutional affiliations.

Authors and Affiliations

Mamoun S. M. Abd El-Kareem¹ · Mohamed A. Rabbih¹ · A. M. Rashad² · Mervat EL-Hefny³ 

✉ Mamoun S. M. Abd El-Kareem
mamoun_sarhan@yahoo.com

✉ Mervat EL-Hefny
mervat.mohamed@alexu.edu.eg

Mohamed A. Rabbih
m.a.rabbih@gmail.com

A. M. Rashad
rashad119@yahoo.com

¹ Molecular and Atomic Physics Unit, Experimental Nuclear Physics Department, Nuclear Research Centre, Egyptian Atomic Energy Authority, Cairo, Inshas, Egypt

² Accelerators and Ion Sources Department, Nuclear Research Centre, Egyptian Atomic Energy Authority, Cairo, Inshas, Egypt

³ Department of Floriculture, Ornamental Horticulture and Garden Design, Faculty of Agriculture (El-Shatby), Alexandria University, Alexandria 21545, Egypt